Institute of Paper Science and Technology
Atlanta, Georgia

IPST TECHNICAL PAPER SERIES

NUMBER 350

AN INVESTIGATION OF BOILING HEAT TRANSFER

IN FIBROUS POROUS MEDIA

GARY R. RUDEMILLER AND JEFFREY D. LINDSAY

FEBRUARY, 1990

AN INVESTIGATION OF BOILING HEAT TRANSFER
IN FIBROUS POROUS MEDIA

GARY R. RUDEMILLER AND JEFFREY D. LINDSAY

NOTICE & DISCLAIMER

AN INVESTIGATION OF BOILING HEAT TRANSFER IN FIBROUS POROUS MEDIA

Gary R. Rudemiller* and Jeffrey D. Lindsay

Engineering Division
The Institute of Paper and Science Technology
Atlanta, GA

*Present address: Westvaco Corporation, Fine
Papers Division, P.O. Box 278, Wickliffe, KY 42087

AN INVESTIGATION OF BOILING HEAT TRANSFER IN FIBROUS POROUS MEDIA

Gary R. Rudemiller* and Jeffrey D. Lindsay

Engineering Division
The Institute of Paper Science and Technology
Atlanta, GA

Boiling phenomena are investigated in the presence of porous media composed of ceramic fibers ranging in diameter from 3.0 to 18.5 μm for system pressures ranging from 0.18 to 0.28 MPa. Bed porosities range from 0.935 to 0.95, average pore diameters range from 30 to 250 μm, and permeabilities range from 2×10^{-11} to 6×10^{-9} m^2. For surface temperatures up to 400°C, measured boiling curves for water in the different fiber beds show maximum heat fluxes on the order of 25 W/cm^2.

The boiling curves exhibit two distinct regimes - a nucleate-type regime and a constant heat flux regime. In the nucleate-type regime, heat flux is directly related to wall superheat, and the slope is directly related to the average pore diameter of the bed. In the constant flux regime, heat flux is independent of wall superheat, as heat transfer is governed by the rate at which the fiber bed supplies water to the heater surface. The transition region can exhibit a peak heat flux and associated rapid escalation in surface temperature similar to burnout in classical pool boiling.

Correlations based on dimensional analysis are presented for both regimes. Data in the constant flux regime are fitted to $\pm$ 35%, but data in the nucleate-type regime are only fitted to $\pm$ 175%.

1. INTRODUCTION

Since the early 1970's, there have been many efforts to improve dewatering capabilities in the papermaking process. The novel process of impulse drying has elicited attention because of its potential to reduce energy costs and improve paper properties. In impulse drying, a moist sheet is pressed against a felt as in conventional wet pressing, but now the pressing surface is heated to 200 to 350°C. This induces an intense dewatering process that gives significantly higher dryness than wet pressing while using less energy than conventional cylinder drying.

The mechanisms that control dewatering during impulse drying appear to differ significantly from those of conventional pressing and drying operations. Both experimental and computational studies suggest that the key to impulse drying is a vapor-liquid displacement mechanism driven by vapor pressure in the sheet (Zavaglia and Lindsay, 1989; Lindsay, 1989). Phase-change heat transfer thus plays an important role. As illustrated in Figure 1, heat transferred to the moist web of paper during impulse drying peaks at instantaneous heat fluxes on the order of 3.0 MW/m^2 (Lavery, 1988). The displacement-augmented dewatering process yields sheet solids contents prior to the dryer section ranging from 55 to 70%. Though most of the water is removed as liquid, a small portion is evaporated, leaving the sheet in vapor form.

Impulse drying is a complex process: in a brief time span

*Present address: Westvaco Corporation, Fine Papers Division, P.O. Box 278, Wickliffe, KY 42087
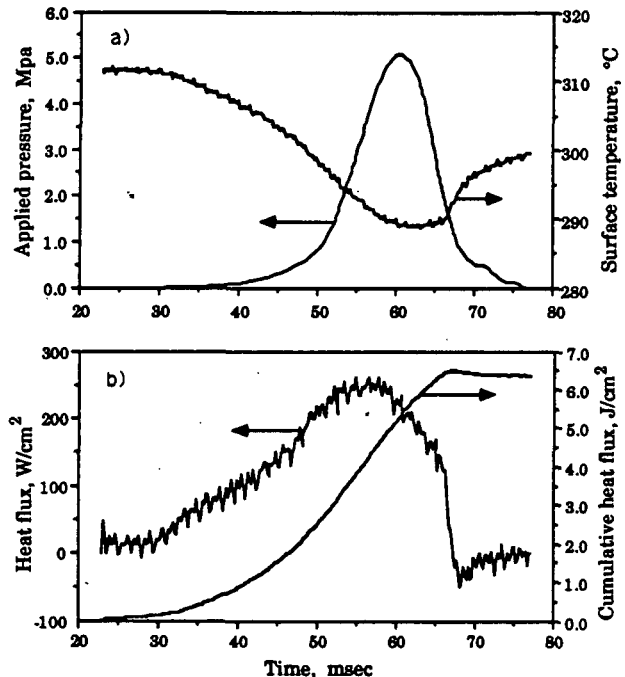
Figure 1. Typical impulse drying data: a) applied pressure and surface temperature, b) heat flux data

(20-100 msec), sheet compression, multiphase flow through porous media, moving phase boundaries, thermodynamics, and boiling heat transfer all interact in complex ways. This research focuses on one idealized aspect of this complex process – boiling heat transfer in fibrous media – in hopes of better understanding the fundamentals of impulse drying.

1.1. Background

Boiling in the presence of liquid-saturated porous media has technological applications in the areas of high-flux heat transfer surfaces, heat pipes, post-accident heat removal from liquid-cooled nuclear reactors, and heat recovery from geothermal reservoirs. Many recent studies in the generic area of boiling in porous media address the convective patterns and two-phase flow phenomena within the porous bed which are induced by boiling at heat fluxes less than 5 W/cm^2 (Sondergeld and Turcotte, 1977; Sondergeld and Turcotte, 1978; Schubert and Strauss, 1979; Abe, et al., 1982; Bau and Torrance, 1982; Bau and Torrance, 1982; Udell, 1985). The porous beds are typically composed of glass beads or silica sand with average diameters ranging from 0.1 to 1.1 mm, have permeabilities ranging from 1×10^{-11} to 140×10^{-11} m^2 and porosities ranging from 0.33 to 0.42, and are from 10 to 20 cm in

1

height. Despite the differences between the bed properties, certain phenomena are consistent among the studies. After phase change commences, a nearly isothermal two-phase zone develops whereby the vapor rises due to buoyant forces and a vapor pressure gradient, and liquid flows down to the heater surface under the influence of capillary forces and gravity. Heat transfer occurs by the counterpercolation of the vapor and liquid phases. Accordingly, the convective two-phase heat transfer is usually modeled as a one-dimensional, isothermal zone with counterflow of liquid and vapor (Torrance, 1983).

The effects of porous media on the mechanism of boiling heat transfer phenomena have been investigated for a number of different media/surface configurations (Costello and Redeker, 1963; Cornwell, et al., 1976; Rannenberg and Beer, 1980; Baum and Greaney, 1981; Abramenko, et al., 1982; Fukusako, et al., 1983; Fukusako, et al., 1986; Chuah and Carey, 1987). Typically, the porous medium is composed of small spheres of various materials, or of fibrous wicking materials, particularly for studies of heat pipes. The results of these varied studies indicate that the nature of the characteristic boiling curve depends on some measure of the pore size in the media, which is easily manipulated by adjusting media particle size. Because of difficulty in adequately characterizing the unique nature of a porous medium, dimensional analysis is frequently used to correlate the heat flux data.

Controlling phenomena for boiling in a porous medium appear to depend on the properties of the medium. However, the available information, most often for boiling in porous media composed of spherical particles, spans only a limited range of surface temperature. To achieve a better understanding of the role of boiling heat transfer in impulse drying, this research addresses the effects of a fibrous medium possessing significant capillary forces on the characteristic boiling curve over a broad range of surface temperature.

2. EXPERIMENTAL APPARATUS

The experimental apparatus designed to gather data for boiling of water in a fibrous medium, illustrated in Figure 2, is discussed in detail elsewhere (Rudemiller, 1989; Rudemiller and Lindsay, 1989). Briefly, the boiling cell apparatus is composed of four systems: the boiling cell, the heat supply system, the data acquisition system, and the process control system. The apparatus is designed to study heating block surface temperatures up to 400°C and cell pressures ranging from 0.10 to 0.28 MPa. The beds are made of ceramic fibers with diameters of 3.0, 8.4, or 18.5 μm. Bed porosity ranges from 0.93 to 0.96, permeability ranges from 10^{-11} to 10^{-9} m², and average pore diameter ranges from 30 to 250 μm.

The boiling cell consists of a 9-cm ID x 110-cm long machined quartz cylinder. The fiber bed is formed in one end of the tube by filtration from a slurry of approximately 0.1% consistency. The tube is axially compressed between the heating block and a top mounting plate to seal the system for pressurized boiling.

The heating block, which is machined from a copper-tellurium alloy (ASTM B145), is 17.8 cm in length by 10.2 cm in diameter. Heat flow from nine cartridge heaters positioned symmetrically in a vertical orientation in the bottom of the heating block is metered by a silicon-controlled rectifier (SCR) based on the output signal from the surface temperature controller. Three thermocouples embedded within the block proximate to the boiling surface measure the temperatures necessary to calculate surface temperature and heat flux based on the one-dimensional heat diffusion equation incorporating a curve-fitted expression for temperature-dependent thermal conductivity of the block. An analog watt transducer measuring power supply to the cartridge heaters verified the accuracy of the technique for calculating heat flux.
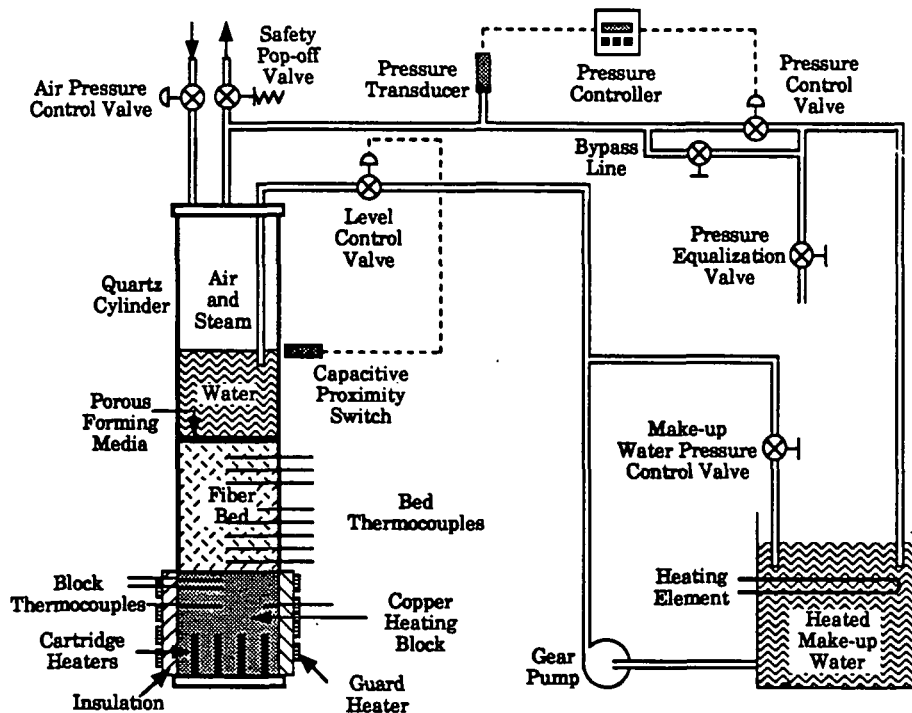

Figure 2. Schematic of the boiling cell apparatus.

The experimental control system developed for this apparatus provides data acquisition, heater block surface temperature control, and system pressure control. A number of type-K thermocouples and one strain-gage pressure transducer are interfaced with PID controllers and a computerized data acquisition system. Software was written to execute a steady-state boiling experiment.

3. RESULTS AND DISCUSSION

The effects of medium pore diameter and system pressure on the boiling curve are determined from boiling experiments in fibrous media. In accordance with standard convention for boiling heat transfer data, log-log axes are chosen to graphically present the experimental data for this study. (With linear axes, the heat flux data exhibit a nearly linear dependence on wall superheat for all boiling regimes in this study.) Based on the additive uncertainty model, the uncertainty for calculated heat flux is 0.9 W/cm^2, and for calculated surface temperature is 0.6°C, both of which are independent of wall superheat. Though the maximum pressure of 0.28 MPa used in this study is probably much lower than levels that develop within the cellulose fiber sheet during impulse drying, a catastrophic failure of the boiling cell at elevated temperatures at 0.28 MPa precluded boiling at higher pressures.

3.1. Qualitative Description of the Phenomena

Once phase-change commences, vapor generated at the heater surface rises under the influence of a partial pressure gradient and buoyant forces, and liquid flows down to the heater surface under the influence of capillary forces and gravity. This two-phase zone of counterpercolating vapor and liquid is nearly isothermal, is at the saturation temperature for the system pressure, and grows in height with heat flux. The vapor condenses at the interface with the overlying liquid-saturated zone. If the height of this zone grows to encompass the entire bed, the vapor protrudes from the top of the bed and agitates the overlying pool of liquid. Fibrous beds as high as 25 cm can become fully engulfed in two-phase flow.

The nature of boiling is modified by the presence of the fibrous bed, as illustrated in Figure 3 (only the nucleate regime of the pool boiling curve for water is presented). The boiling curve for the fibrous bed exhibits two boiling regimes and a point of transition between them that represents the peak heat flux attained during the experiment. The direct dependence of heat flux on wall superheat in the initial regime is similar to the nucleate pool boiling regime. Heat transfer is limited by

the ability of the heater to supply heat, which is related to nucleation characteristics of the heater surface. Apparently, some form of active nucleation is occurring at voids on the heater surface, within limits posed by physical constraints of the pore structure. Physical inhibition of nucleation may account for the reduced nucleate boiling effectiveness demonstrated with the fibrous medium. It is during this nucleate-type regime that the isothermal, two-phase counterpercolation zone develops.

In the second regime, the heat flux is totally independent of wall superheat. Here, heat flux is apparently controlled by the rate of liquid flow to the heater surface under the influence of capillary forces of the bed. This depends on the saturation level and pore size distribution of the bed. Development of a vapor film on the heater surface in this regime is unlikely because the inertial force of the liquid flowing to the surface would break through the film. Consequently, some degree of liquid/surface contact is likely to occur throughout this regime, which means that phase change may occur by nucleation throughout the entire boiling curve.

The point of transition between the two regimes, called the transitional heat flux (THF), can exhibit moderate instability. Beds with average pore diameters greater than 220 µm exhibit a peak heat flux that has a magnitude greater than that of the constant heat flux. At the THF, a dramatic change in the fluid flow phenomena reduces the heat-absorbing capacity of the bed. Attempts to increase surface temperature beyond the THF yield a rapid rise in surface temperature (typically, an increase of 10 to 15°C in a period of 10 to 15 seconds) until the surface temperature control system arrests the rise.

Saturation is undoubtedly a major factor in controlling heat flux, particularly in the constant flux regime. The observation of a peak heat flux and subsequent decline to constant flux for beds of large average pore diameter may be related to the saturation profile. This decline is postulated to be caused by a reduction in the ability of the bed to supply water to the heater surface. Since the pore structure of the rigid bed is unchanged, something must happen to change the saturation profile in the bed at the THF. Due to volume expansion upon phase-change, the velocity of vapor in the flow channels is likely to be much higher than that of liquid. In a manner analogous to the Helmholtz instability at the interface of two immiscible fluids, the vapor velocity in the flow channels may reach a critical level that effects a change in the relative distribution of water and vapor phases within the bed.

The Effect of Average Pore Diameter. The average pore diameter of the bed significantly influences boiling phenomena, as illustrated in Figure 4. The slope of the nucleate-type regime decreases as pore diameter decreases, most probably
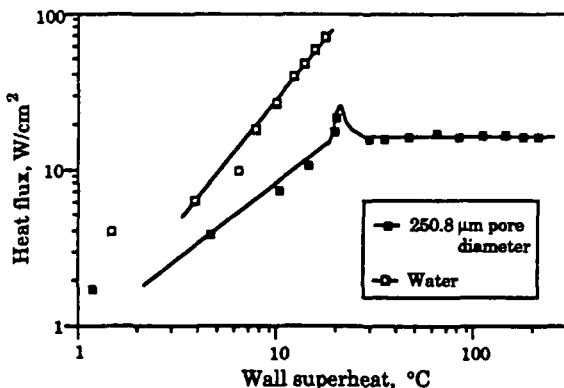
Figure 3. Typical measured boiling curves. Fiber diameter was 18.5 µm, porosity was 0.946, and permeability was 5.4x10^{-10}m^2
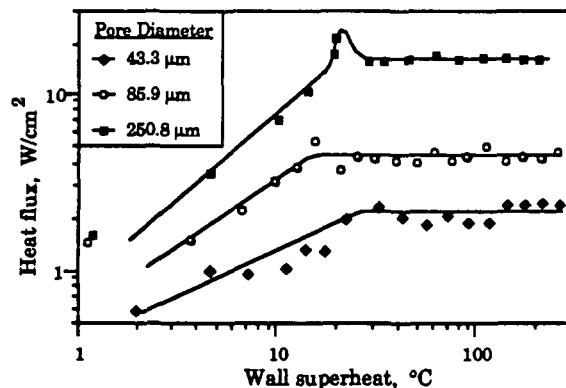
Figure 4. The effect of average pore diameter on the boiling curve at atmospheric pressure.

because of the effects on the hydrodynamics of the vapor phase. Nucleation is probably inhibited, and the resistance to vapor flow away from the heater surface increases in proportion to the diameters of the flow channels. Any accumulation of vapor at the surface will increase the resistance to heat transfer at the surface.

Behavior at the THF depends on the average pore diameter of the bed as well. Each boiling curve for the large average-pore-diameter beds (220 to 260 μm) exhibits a distinct peak in heat flux between the two boiling regimes with an associated rapid escalation in surface temperature. However, the small average-pore-diameter beds (35 to 90 μm) exhibit a smooth transition. This difference in behavior at the THF may be related to the curvature of the saturation profile in the bed.

The magnitude of heat flux in the constant heat flux regime is directly related to average pore diameter. Obviously, as the pore diameters in a given type of porous medium decrease, the permeability decreases, thus lowering both the rate of liquid supply to the surface and also lowering the steady-state phase-change heat flux.

The Effect of System Pressure. Figure 5 illustrates the effect of system pressure on the boiling curves for fibrous beds with average pore diameters of approximately 250 μm. Prior to the region of transition, the nucleate-type regime is insensitive to pressure in the studied range. The effects of a higher bed saturation due to the increased vapor phase density at elevated pressures are not apparent in the heat flux data in the nucleate-type regime below wall superheats of about 20°C. This suggests that geometric constraints dominate pressure effects in controlling nucleation. The nucleate-type regime for beds with average pore diameters less than 90 μm also do not appear to be affected by pressure.
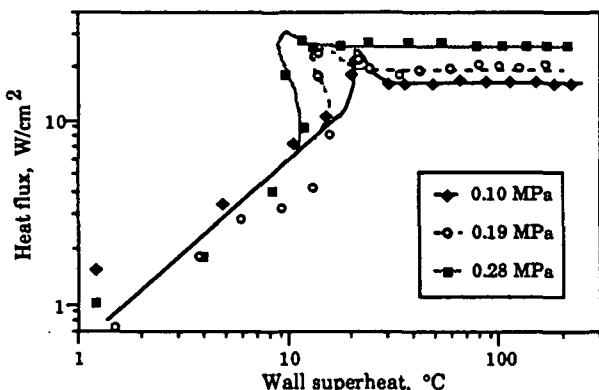

Figure 5. The effect of system pressure on the boiling curve.

For beds with large average pore diameters, process instability at the THF is exacerbated as the system pressure increases. As the THF is approached, the relationship between wall superheat and heat flux reverses: the wall superheat actually decreases as higher heat fluxes are approached. This is exhibited as a backward bend in the boiling curve, until finally, the heat flux peaks and the surface temperature rapidly escalates. The behavior of decreasing wall superheat at increased levels of heat flux just prior to the critical is reproduced in all of the pressurized boiling runs for beds with average pore diameters above about 220 μm. The wall superheat at the THF is inversely proportional to pressure, which agrees with the trend observed in classical pool boiling (Cichelli and Bonilla, 1945).

The effect of pressure on the heat flux in the constant flux regime is in part due to the increased density of the vapor phase. The consequent increase in bed saturation results in greater liquid water supply to the heater surface, which

increases the heat-absorbing capacity of the bed. For all average pore diameters, the magnitude of the constant heat flux under pressure is greater than that for atmospheric conditions.

3.2. Correlation of the Boiling Data

The Buckingham Pi Theorem is used to develop meaningful dimensionless groups for this physical system with which dimensionless correlations are developed. For correlation purposes, the data have been segregated into two groups according to boiling regime. Each correlation is developed from a stepwise regression using appropriate F-statistics, and each correlation is tested for lack of fit.

Though twelve dimensionless groups were used in stepwise regression, statistically significant dimensionless groups for this study are limited to the Reynolds number (Re), the Jakob number (Ja), the constant heat flux number (N_{cf}), and the geometric scale factor (Λ). The definition of Re,

$$Re = \frac{q\,\overline{D}}{h_{lv}\,\eta_l\,\varepsilon} \quad , \qquad (1)$$

follows the convention introduced by Rannenberg and Beer (1980). The average pore diameter of the bed is chosen as the characteristic length of the system. Greater statistical significance of the correlations is achieved by non-dimensionalizing the heat flux according to this definition of Re rather than by using a Nusselt number. Additionally, the lack of dependence of heat flux on wall superheat in the constant heat flux regime diminishes the physical significance of a Nusselt number. N_{cf} appears to be a unique group that represents the competing forces of viscosity of the liquid phase and capillarity, defined as

$$N_{cf} = \eta_l^2 / \overline{D}\,\rho_l\,\sigma \quad . \qquad (2)$$

The ranges of these groups for this research are as follows: Re ranges from 2.105×10^{-4} to 0.1606, Ja ranges from 4.715×10^{-4} to 0.589, N_{cf} ranges from 3.51×10^{-6} to 3.45×10^{-5}, and Λ ranges from 2.79×10^{-4} to 2.94×10^{-3}. No attempt is made to correlate the THF due to insufficient data.

The Constant Flux Regime. Because heat flux is completely independent of wall superheat in the constant heat flux regime, the heat flux data of each boiling curve are averaged to reduce the number of data points in the correlation. The correlation for the constant flux regime,

$$\frac{q\,\overline{D}}{h_{lv}\,\eta_l\,\varepsilon} = 7.161 \times 10^{-11} \left(\frac{\eta_l^2}{\overline{D}\,\rho_l\,\sigma}\right)^{-1.861} \left(\frac{\overline{D}}{H}\right)^{0.296} \quad , \qquad (3)$$

which fits the data to ± 11.5% on average and ± 35% peak-to-peak, is illustrated in Figure 6; normalized residuals are illustrated in Figure 7. This correlation supports the supposition that the ability of the bed to supply water to the heating surface is the controlling mechanism for this regime. The statistical significance of the geometric scale factor reflects the importance of the thickness of the medium.

The Nucleate-type Regime. Because the nucleate-type regime demonstrates a direct dependence on wall superheat, all data points are retained for the correlation. Stepwise regression yields the following correlation:

$$\frac{q\,\overline{D}}{h_{lv}\,\eta_l\,\varepsilon} = 2.838 \times 10^{-10} \left(\frac{C_{p_l}\,\Delta T_w}{h_{lv}}\right)^{0.703} \left(\frac{\eta_l^2}{\overline{D}\,\rho_l\,\sigma}\right)^{-1.744} \quad . \qquad (4)$$
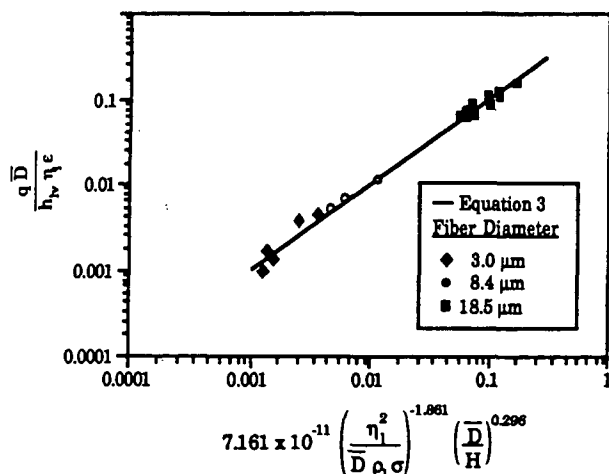
4

Figure 6. Dimensionless correlation for the constant heat flux regime.

$$7.161 \times 10^{-11} \left(\frac{\eta_l^2}{\overline{D} \rho_l \sigma}\right)^{-1.861} \left(\frac{\overline{D}}{H}\right)^{0.296}$$

Figure 8. Dimensionless correlation for the nucleate-type regime.

$$2.838 \times 10^{-10} \left(\frac{C_{p_l} \Delta T_w}{h_{lv}}\right)^{0.703} \left(\frac{\eta_l^2}{\overline{D} \rho_l \sigma}\right)^{-1.744}$$

Figure 7. Normalized residuals for the constant flux regime.
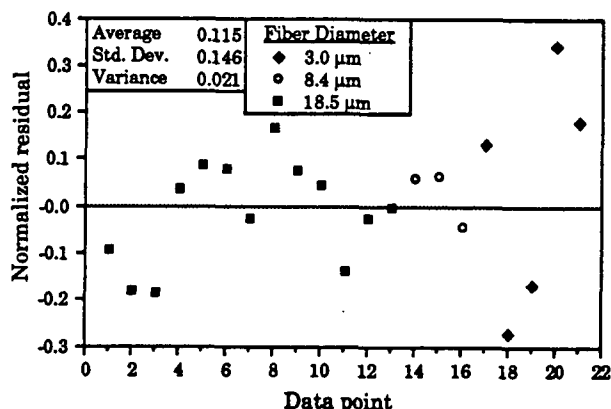

Figure 9. Normalized residuals for the nucleate-type regime.

The correlation, which fits the data to ± 37.0% on average and ± 175% peak-to-peak, is shown in Figure 8, and normalized residuals are shown in Figure 9. Though this correlation represents the data, its accuracy as a tool for predicting nucleate-type regime heat flux is severely limited. Normalized residuals as high as 175% indicate that the correlation can at best be used to predict trends. The inaccuracy of this correlation partially stems from the inability to incorporate surface nucleation characteristics into the correlation. The appearance of the constant heat flux number underscores the importance of the medium's ability to transport liquid to the surface.

Comments on the Correlations. Neither of the statistically-significant correlations explicitly reflects the effects of fiber diameter or of vapor density, though it is apparent from the data that each is important to the observed phenomena. The dependence on fiber diameter is, however, implicitly incorporated through the average pore diameter of the bed. Complicated correlations have been developed to express the average pore diameter of the beds in this study as a function of fiber diameter, fiber length, and bed porosity (Rudemiller, 1989).

Considering the effect of magnitude of system pressure on the heat transfer phenomena, the absence of vapor-phase density in the correlations is surprising. Attempts to correlate the data with dimensionless groups based on physical properties of vapor evaluated at the appropriate system pressure and saturation temperature yielded no improvement in statistical significance compared to Equations 3 and 4. This suggests that
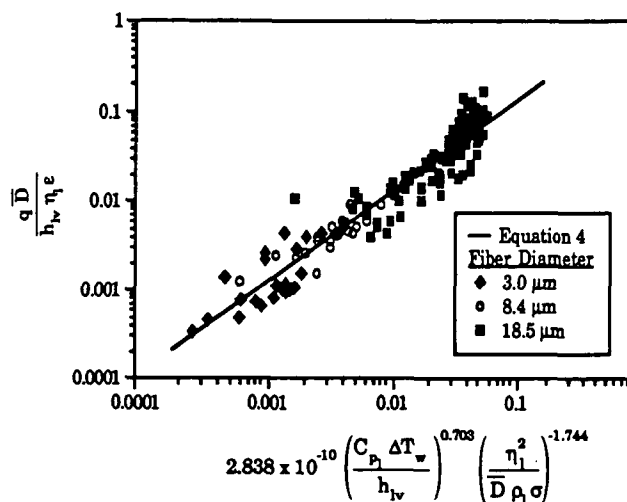
pressure dependence is modeled by accounting for the physical properties of the liquid phase. Additional correlations developed from dimensionless groups based on physical properties of liquid evaluated at atmospheric pressure also failed to yield an improved statistical significance. Consequently, dimensionless groups based on physical properties of liquid adequately model the pressure dependence of the phenomena.

4. CONCLUSIONS

Boiling in the presence of a fibrous porous medium exhibits phenomena that differ from classical pool boiling. Boiling curves in a fibrous bed show two regimes. The first regime is similar to the nucleate regime of classical pool boiling in that heat flux is directly proportional to wall superheat. Heat transfer in this nucleate-type regime is probably controlled by nucleation characteristics of the heater surface and physical space available for vapor growth. The heat flux of the second regime is constant. Heat transfer is then controlled by the rate at which the pores of the fibrous bed supply water to the heater surface.

The average pore diameter of the bed is an important factor for boiling in a fibrous medium. The slope of the nucleate-type regime, and the magnitude of heat flux in the constant heat flux regime, are directly proportional to the average pore diameter. The behavior at the point of transition

appears to depend on a critical value of average pore diameter, as beds with pore diameters above 220 μm exhibit a peak, while beds with pore diameters below 90 μm have a smooth transition. System pressure apparently has no effect on the portion of the nucleate regime prior to the transition region. However, at elevated pressures, the instability exhibited by the large-pore-diameter beds at the THF is exacerbated. The heat flux in the constant flux regime increases with pressure as the decrease in vapor density yields higher levels of bed saturation.

5. ACKNOWLEDGMENTS

6. NOMENCLATURE

g - gravitational acceleration
C_p - specific heat
$\overline{D}$ - average pore diameter
h - height in capillary
h_{lv} - latent heat of vaporization
H - bed height
k_{eff} - effective thermal conductivity
r - radius of capillary
t - time
ΔT_w - wall superheat

Greek Letters
ε - porosity
η - viscosity
θ - contact angle
ρ - density
σ - surface tension

Subscripts
l - liquid
v - vapor

Dimensionless Groups

Constant heat flux number, $N_{cf} = \eta_L^2 / \overline{D}\rho_L\sigma$

Geometric scale factor, $\Lambda = \overline{D}/H$

Jakob number, $Ja = C_{p_l} \Delta T_w / h_{lv}$

Reynolds number, $Re = q\overline{D} / h_{lv}\eta_l \varepsilon$

7. BIBLIOGRAPHY

1. Abe,T., Eckert, E.R.G., & Goldstein, R.J. 1982, A Parametric Study of Boiling in a Porous Bed, Thermo- and Fluid Dynamics, vol. 16, pp.119-126.
2. Abramenko, A.N., Kanonchik, L.E., Shaskov, A.G., & Sheleg, V.K. 1982, Heat Transfer with Evaporation and Boiling of a Liquid in Porous Bodies, J. Eng. Physics, vol. 42, pp. 144-150.
3. Bau, H.H., & Torrance, K.E. 1982, Boiling in Low-Permeability Porous Materials, Int. J. Heat and Mass Transfer, vol. 25, pp. 45-55.
4. Bau, H.H., & Torrance, K.E. 1982, Thermal Convection and Boiling in a Porous Medium, Let. Heat Mass Transfer, vol. 9, pp. 431-441.
5. Baum, A.J., & Greaney, P.K. 1981, An Experimental and Analytical Investigation of Boiling Heat Transfer in Porous Bodies, 20th Joint ASME/AIChE National Heat Transfer Conference, Milwaukee, WI, August 2-5, pp. 1-9.
6. Cichelli, M.T. & Bonilla, C.F. 1945, Heat Transfer to Liquids Boiling Under Pressure, Trans. AIChE. vol. 41, pp. 755-787.
7. Cornwell, K., Nair, B.G., & Patten, T.D. 1976, Observation of Boiling in Porous Media, Int. J. Heat and Mass Transfer, vol. 19, pp. 236-238.
8. Costello, C.P., & Redeker, E.R. 1963, Boiling Heat Transfer and Maximum Heat Flux for a Surface with Coolant Supplied by Capillary Wicking, AIChE Chem. Eng. Progress Symp. Series, vol. 59, no. 41, pp. 104-113.
9. Chuah, Y.K., & Carey, V.P. 1987, Boiling Heat Transfer in a Shallow Fluidized Particulate Bed, J. Heat Transfer, vol. 109, pp.196-203.
10. Fukusako, S., Seki, N., & Komoriya, T. 1983, An Experimental Study of Boiling Heat Transfer in a Water-Saturated Porous Bed, ASME-AIChE Thermal Engineering Joint Conf. Proceedings, Honolulu, HI, pp. 167-173.
11. Fukusako, S., Komoriya, T., & Seki, N. 1986, An Experimental Study of Transition and Film Boiling Heat Transfer in a Liquid-Saturated Porous Bed, J. Heat Transfer, vol. 108, pp. 117-124.
12. Lavery, H.P. 1988, High-Intensity Drying Processes - Impulse Drying, Report Three, U.S. Department of Energy Contract No. FG02-85CE40738.
13. Lindsay, J. D. 1989, The Physics of Impulse Drying: New Insights from Numerical Modeling, Fundamentals of Papermaking, Transactions of the Ninth Fundamental Research Symposium, Cambridge, England, ed. C. F. Baker and V. W. Punton, vol. 2, pp. 679-729, Mechanical Engineering Publications, London.
14. Rannenberg, M., & Beer, H. 1980, Heat Transfer by Evaporation in Capillary Porous Wire Mesh Structures, Let. Heat Mass Transfer, vol. 7, pp. 425-436.
15. Rudemiller, G.R. 1989, A Fundamental Study of Boiling Heat Transfer Mechanisms Related to Impulse Drying, Ph.D. thesis, The Institute of Paper Science and Technology, Atlanta, GA.
16. Rudemiller, G.R., & Lindsay, J.D. 1989, Apparatus for Investigating Boiling Phenomena in a Fibrous Porous Medium, Int. Comm. Heat Mass Transfer, vol. 16, pp. 785-794.
17. Schubert, G., & Straus, J.M. 1979, Steam-Water Counterflow in Porous Media, J. of Geophys. Res., vol. 84, pp. 1621-1628.
18. Sondergeld, C.H., & Turcotte, D.L. 1977, An Experimental Study of Two-Phase Convection in a Porous Medium with Applications to Geological Problems, J. of Geophys. Res. vol. 82, pp. 2045-2053.
19. Sondergeld, C.H., & Turcotte, D.L. 1978, Flow Visualization Studies of Two-Phase Thermal Convection in a Porous Layer, Pure Applied Geophys. vol. 117, pp. 321-330.
20. Torrance, K.E. 1983, Boiling in Porous Media, ASME/JSME Thermal Eng. Joint Conf. Proceedings, Honolulu, HI, March 20-24, vol. 2., pp. 593-606.
21. Udell, K.S. 1985, Heat Transfer in Porous Media Considering Phase Change and Capillarity - The Heat Pipe Effect, Int. J. Heat Mass Transfer, vol. 28, pp. 485-495.
22. Zavaglia, J. C., & Lindsay, J. D. 1989, Flash X-ray Visualization of Multiphase Flow During Impulse Drying, Tappi J., vol. 72, no. 9, pp.79-85.